

Orbit Determination of Highly Elliptical Earth Orbiters Using Improved Doppler Data-Processing Modes

J. A. Estefan
Navigation Systems Section

A navigation error covariance analysis of four highly elliptical Earth orbits is described, with apogee heights ranging from 20,000 to 76,800 km and perigee heights ranging from 1,000 to 5,000 km. This analysis differs from earlier studies in that improved navigation data-processing modes were used to reduce the radio metric data. For this study, X-band (8.4-GHz) Doppler data were assumed to be acquired from two Deep Space Network radio antennas and reconstructed orbit errors propagated over a single day. Doppler measurements were formulated as total-count phase measurements and compared to the traditional formulation of differenced-count frequency measurements. In addition, an enhanced data-filtering strategy was used, which treated the principal ground system calibration errors affecting the data as filter parameters. Results suggest that a 40- to 60-percent accuracy improvement may be achievable over traditional data-processing modes in reconstructed orbit errors, with a substantial reduction in reconstructed velocity errors at perigee. Historically, this has been a regime in which stringent navigation requirements have been difficult to meet by conventional methods.

I. Introduction

The principal focus of recent navigation-related research has been on the development of new or improved navigation techniques to simultaneously improve performance, while reducing navigation-related requirements levied upon spacecraft and associated mission operations. The motivation for such a focused effort is clear—tighter budgetary constraints imposed on current and future NASA space science missions. Advanced studies of interplanetary mission scenarios have shown that medium-to-high navigation accuracies (40 to 15 nrad in an angular sense) can be achieved through the use of nontraditional data-processing modes for Doppler and ranging data types acquired from the Deep Space Network (DSN) [1,2]. These new techniques take advantage of improved calibrations of the limiting ground system error sources affecting the data and make use of high-speed workstation computers to reduce the data. Studies are also being conducted to demonstrate the utility of these alternative data-processing modes with actual flight data acquired from the Ulysses and Galileo spacecraft [3,4].

These promising research findings prompted this investigation into the use of improved radio metric data-processing modes in tracking and navigational support of high Earth orbiter (HEO) missions. In this

article, a navigation error covariance analysis is described, which studies the utility of advanced data-processing modes for X-band (8.4-GHz) Doppler data acquired from DSN-based radio antennas. The analysis investigates two-way Doppler-only navigation performance; other radio metric data strategies, such as two-way radio ranging, are not addressed. A discussion of Doppler data-processing modes is presented along with assumptions for error covariance analysis derived from an improved set of data acquisition and orbit determination error-modeling strategies. Results from the covariance analysis are described for four sample highly elliptical orbits of the space very long baseline interferometry (SVLBI) mission set. A discussion section highlights some critical implications from the analysis and areas that will require further investigation.

II. Doppler Data-Processing Modes

A. Phase Versus Frequency

DSN Doppler data acquired in a two-way coherent mode are not direct frequency shift measurements, but integral counts of the number of cycles of the transmitted carrier signal relative to the received carrier signal that have accumulated over a tracking pass [1]. These cycle counts are differenced to form measurements of the average Doppler shift over short time intervals (typically 1 to 10 min); it is these *differenced-count Doppler* measurements that have traditionally been used for navigating spacecraft [5].¹ The purpose of differencing the Doppler counts was to overcome limitations in early tracking hardware that caused discontinuities in the data (known as *cycle slips*) that occurred when the ground receiver's phase-tracking loop would momentarily lose its lock on the spacecraft carrier signal. Cycle slips are most likely to occur when the spacecraft's Doppler frequency is large and varies rapidly or when the spacecraft carrier signal-to-noise ratio approaches the tracking threshold of the ground receiver.

The notion of using the original Doppler count as a navigation measurement was considered as early as 1966 by Curkendall [6], but the idea was not popularized because of the operational constraints cited above. Given the steady improvements in the DSN tracking system over the years, together with the development of robust methods for resolving occasional cycle slips, there is a renewed interest in using the original Doppler count (subsequently referred to as *total-count phase*) as a viable data type for spacecraft navigation [1].² The motivation for using total-count phase as a navigation measurement is that the precision of these data is very high (a few millimeters at X-band frequencies) whereas differencing cycle counts to construct a frequency-formulated observable effectively increases the data noise level. Furthermore, unlike Doppler that is differenced-count formulated, phase-formulated Doppler lends itself to a simpler data noise model since the errors are uncorrelated.

B. Filtering Strategies

The standard orbit determination filtering strategy used by flight project navigation teams treats various systematic error sources as unmodeled *consider* parameters, which are not estimated but whose effects are accounted for (i.e., "considered") in computing the error covariance of filter (estimated) parameters [7]. In a consider state analysis, the estimated parameter set's sensitivity to various unmodeled consider parameters can be computed via the partial derivatives of the state estimate with respect to the consider parameter set [8]. Depending on the magnitude of the resulting sensitivities, the filter-computed estimation error covariance is modified to account for unmodeled effects to generate a more realistic estimate of predicted navigation performance. The filter has no knowledge of the unmodeled parameters'

¹ Historically, the result of differencing cycle counts to form measurements of the average Doppler shift has been referred to as *differenced-range Doppler*, the convention originating from the mathematical formulation of the observable in which the station-to-spacecraft range is explicitly differenced over a specified integration, or "count," time.

² T. D. Moyer, "ODE and REGRES Modifications for Processing Block V Receiver Doppler Observables and Total Count Phase Observables," JPL Engineering Memorandum 314-568 (internal document), Jet Propulsion Laboratory, Pasadena, California, August 24, 1993.

contribution to uncertainty in the state estimate since the modified covariance (the consider covariance), including effects from both the estimated and consider parameters, is not fed back to the filter.

Some principal reasons for using a consider state filter are: (1) certain parameters, such as fiducial station locations, may be fixed in order to define a reference frame and/or length scale; (2) there may be a lack of adequate models for an actual physical effect; (3) computational limitations exist when attempting to adjust parameters of high order, such as the coefficients in a gravity field; or (4) if estimated, the computed uncertainty in model parameters would be reduced far below the level warranted by model accuracy [9,10]. Consider state filters have been known to experience failure modes, such as when additional data yield an increase in the consider covariance, or when the consider covariance propagates to an unreasonably large result over time [10]. In these instances, it is usually necessary to empirically “tune” the filter by adjusting data weights or model assumptions to obtain useful estimates.

A new sequential data-filtering strategy currently under study is the enhanced orbit determination filter, in which most or all of the major systematic ground-system calibration error sources affecting the data are treated as filter parameters, along with spacecraft trajectory parameters [1,11,12]. This strategy differs from current practice, in which the ground-system calibration error sources are represented as unestimated bias or consider parameters and accounted for only when computing the error covariance of the filter parameters. The motivation behind the enhanced filter is not so much to improve upon the a priori ground system calibrations, but to incorporate a more accurate model of the physical world into the filter [1].

III. Error Covariance Analysis Assumptions

Earlier orbit determination studies of DSN-based Doppler tracking for HEO missions focused on using the conventional frequency formulation of the Doppler observable along with a standard consider state filtering strategy [13]. For this new study, a revised error covariance analysis was performed to quantify the navigational utility of a phase formulation of the Doppler observable together with an enhanced data-filtering strategy, which treats the principal ground system calibration error sources as filter parameters. In this section, assumptions for the revised navigation error covariance analysis are provided, including orbit characteristics, data-acquisition and simulation strategies, and filter error modeling.

A. Sample Orbits

Four highly elliptical orbits, all derived from the international SVLBI mission set, were selected for analysis. The first orbit represents the current operational orbit design for the Japanese MUSES-B spacecraft of the VLBI Space Observatory Program (VSOP), targeted to launch in September 1996 [14]. Nominal orbit parameters are provided in Table 1. The MUSES-B orbit is the lowest of the four sample orbits, with perigee and apogee heights of 1,000 and 20,000 km, respectively. The second orbit is representative of the latest orbit design for the Russian RadioAstron project [15]. It is the most eccentric of the sample orbits, with perigee and apogee heights of 5,000 and 76,800 km, respectively. Table 2 lists the nominal orbit parameters for RadioAstron, targeted to launch in 1997 or 1998.

The two remaining sample orbits are both based on preliminary orbit designs for the Advanced Radio Interferometry Between Space and Earth (ARISE) SVLBI mission. ARISE is intended to be a next-generation SVLBI mission with a more ambitious set of scientific goals than VSOP and RadioAstron [16]. Current ARISE orbit design calls for perigee and apogee heights of about 5,000 and 12,000 to 50,000 km, respectively; final orbit selection will ultimately depend on the principal scientific objectives of the mission. For this analysis, two candidate orbits were assumed with apogee heights of 12,000 and 50,000 km. Nominal orbit parameters for a mission launch in 2005 are provided in Table 3. Note that ARISE will have very stringent orbit determination requirements that exceed the capability of current and anticipated ground-based radio tracking strategies, such as two-way Doppler, and will require a much more ambitious tracking and navigation strategy. Current design calls for two onboard Global

Table 1. Sample orbit parameters for the Japanese VSOP mission (MUSES-B).

Parameter	Value
Nominal launch date	September 1996
Initial spacecraft ephemeris	
Semimajor axis	16,878 km
Eccentricity	0.5629
Inclination	31.0 deg
Argument of perigee	134.24 deg
Longitude of ascending node	116.14 deg
Mean anomaly	0.0 deg
Additional parameters	
Perigee height	1,000 km
Apogee height	20,000 km
Orbit period	6.06 h

Table 2. Sample orbit parameters for the Russian RadioAstron project.

Parameter	Value
Nominal launch date	1997/98
Initial spacecraft ephemeris	
Semimajor axis	46,778 km
Eccentricity	0.7781435
Inclination	51.5 deg
Argument of perigee	190.0 deg
Longitude of ascending node	300.0 deg
Mean anomaly	0.0 deg
Additional parameters	
Perigee height	4,000 km
Apogee height	76,800 km
Orbit period	28 h

Positioning System (GPS) receivers [16].³ However, for this analysis, it is the orbit characteristics that are of principal interest, not the actual mission requirements.

B. Tracking Data Simulation

Only two passes of two-way Doppler data were simulated from two different DSN sites. The lengths of the data arcs depend on the sample orbit being studied. For shorter orbit periods, such as the MUSES-B 6.06-h orbit, a 2.25-h pass from the Madrid site and a 2.43-h pass from the Canberra site were assumed.

³ S. C. Wu and R. P. Malla, "GPS-Based Precision Determination of Highly Elliptical Orbits for Orbiting VLBI Applications," JPL Interoffice Memorandum 335.8-94-004 (internal document), Jet Propulsion Laboratory, Pasadena, California, March 29, 1994.

Table 3. Sample orbit parameters for the ARISE mission.

Parameter	Value
Nominal launch date	2005
Initial spacecraft ephemeris	
Semimajor axis	18,878.15 km/33,878.15 km
Eccentricity	0.40/0.66
Inclination	60.0 deg
Argument of perigee	0.0 deg
Longitude of ascending node	0.0 deg
Mean anomaly	0.0 deg
Additional parameters	
Perigee height	5,000 km
Apogee height	12,000 km/50,000 km
Orbit period	7.17 h/17.24 h

In the case of the ARISE 7.17-h orbit, a 4.07-h pass from Madrid and a 4.20-h pass from Goldstone were assumed. The two passes for the 28-h RadioAstron orbit consisted of a 3.03-h Goldstone pass and a longer 15.82-h Madrid pass. For the longer 17.24-h ARISE orbit, a 9.52-h Madrid pass and a 4.23-h Goldstone pass were assumed.

To account for random data noise, the measurement error models of [1] were assumed. These models are representative of the DSN’s current X-band Doppler system for the 34-m high efficiency (HEF) stations with nominal values for spacecraft turnaround ratio, transmit frequency of the carrier signal, and sample time. For a differenced-count Doppler measurement at time t_k , denoted as f_k , the following model is assumed:

$$f_k \equiv \dot{\rho}_k + \nu_k \quad (1)$$

where

$\dot{\rho}_k$ = station-to-spacecraft range rate at time t_k

ν_k = samples of a zero-mean white Gaussian sequence, in which each sample has constant variance and is uncorrelated with all other samples⁴

The random process ν incorporates both additive phase-measurement errors and errors due to ground system frequency instability that are integrated over the count time of each observation. For this analysis, differenced-count Doppler measurements were weighted with a $1\text{-}\sigma$ measurement uncertainty of 0.1 mm/s (metric value) for a 60-s count time. In addition, additive noise variances were adjusted by an elevation-dependent function to reduce the weight of the low-elevation data. No data were acquired at elevation angles below 10 deg from any DSN site.

For a total-count phase measurement at time t_k , denoted as ϕ_k to represent the Doppler count at time t_k , the following model is assumed:

⁴This approximation is not rigorously correct since successive differenced-count Doppler data points share common values of the Doppler count and, therefore, each data point is correlated with the two points adjacent to it. In practice, it is believed that the uncorrelated measurement error assumption does not yield significantly incorrect statistical calculations for the large Doppler data sets typically used in mission operations [1].

$$\phi_k \equiv (\rho_k - \rho_0) + \phi_0 + \eta_k + \xi_k \quad (2)$$

where

- ρ_k = station-to-spacecraft range at time t_k
- ρ_0 = station-to-spacecraft range at time t_0
- ϕ_0 = unknown phase offset of Doppler counter at time t_0

and

- η_k = additive phase-measurement error
- ξ_k = cumulative phase-measurement error

The phase offset, ϕ_0 , represents the Doppler counter initialization error and is assumed to be a random bias. The η_k samples are assumed to be a white, zero-mean Gaussian sequence with constant variance, and the ξ_k values represent the cumulative phase error induced by the integration of frequency variations by the Doppler counter. The total-count phase measurements were weighted for this analysis with a $1\text{-}\sigma$ measurement uncertainty of 2.5 mm (metric value).⁵ As with differenced-count Doppler, the additive noise variances were adjusted by an elevation-dependent function to reduce the weight of low-elevation data, and a 10-deg lower elevation cut-off angle assumed for the DSN stations.

C. Orbit Determination Error Model

Table 4 provides the dynamic and observational error model assumptions that make up the enhanced orbit determination filter, along with a priori statistics, steady-state uncertainties for the Gauss–Markov parameters, and noise densities, N , for the random walk parameters. With the exception of the gravitational force model, all parameters were treated as filter parameters and grouped into three categories: spacecraft epoch state, spacecraft nongravitational force model, and ground system error model. The Earth’s gravitational parameter (GM) and geopotential field harmonic coefficients were treated as unmodeled consider parameters and grouped in the gravitational force model category. By comparison, Table 5 gives the error modeling assumptions that comprise the standard consider state filter model.

A batch-sequential factorized Kalman filter was used in the estimation process, with a batch size of 840 min (14 h) for the standard-filtering strategy, reduced to 10-min batch intervals for the enhanced-filtering strategy so that short-term fluctuations could be tracked in the transmission media. For process noise, first-order Gauss–Markov (exponentially correlated) random processes were assumed. The process noise covariance is given by $q = (1 - m^2) \sigma_{ss}^2$ where $m = \exp[-(t_{j+1} - t_j)/\tau]$. Here, t_j is the start time for the j th batch and τ is the associated time constant. The term σ_{ss} is the steady-state uncertainty, i.e., the noise level that would be reached if the dynamical system were left undisturbed for a time much greater than τ . For the random walk, both σ_{ss} and τ are unbounded ($\tau = \infty$) and a steady state is never reached. The noise density for the random walk is characterized by the rate of change of the process noise covariance, $q = \Delta q/\Delta t$, where Δ is the batch size and Δq is the amount of noise added per batch [9].

⁵ The data noise values for both differenced-count Doppler and total count phase can be readily modified for future navigation analyses as the performance specifications of the supporting ground system begin to mature.

Table 4. Enhanced orbit determination filter with ground-system error model representative of current DSN calibration accuracy.

Estimated parameter set	Uncertainty (1σ)	Remarks
Spacecraft epoch state	A priori	Constant parameters
Position	10^3 km	
Velocity	1 km/s	
Nongravitational force model		
Solar radiation pressure	Steady-state	Markov parameters
Specular/diffuse reflectivity	10 percent of nominal	0.25–3 day time constant
Anomalous accelerations	Steady-state	Markov parameters
Radial	10^{-12} km/s ²	1–3 day time constant
Transverse	10^{-12} km/s ²	1–3 day time constant
Ground system error model		
Doppler phase offset (each station)	A priori 100 km	Random walk 1 cm ² /h
DSN station coordinates		
Crust fixed	A priori	Constant parameters
Spin radius (r_s)	0.18 m	
Z-height (z_h)	0.23 m	
Longitude (λ)	3.6×10^{-8} rad	
Geocenter offset Z-component	A priori 1 m	Constant parameters
Earth orientation		
Pole orientation	Steady-state 1.5×10^{-8} rad	Markov parameters 1-day time constant
Rotation period	0.2 ms	12-h time constant
Transmission media		
Zenith troposphere (each station)	A priori 5 cm	Random walk 1 cm ² /h
Consider parameter set	Uncertainty (1σ)	Remarks
Gravitational force model		
Earth’s GM	A priori GM $\times 10^{-8}$	Constant parameters
Harmonics	8×8 field (GEM-L2)	

The principal difference between the enhanced and standard filter models used for this study was the modeling of observational errors, namely:

- (1) A random walk model (simple Brownian motion process) was used to track short-term fluctuations in the troposphere and assumed zenith delay calibration uncertainties representative of the current DSN-based calibration accuracy.
- (2) A phase offset parameter for each station was included in the ground system error model. As with the tropospheric path delays, these parameters were modeled as random walk processes. Table 4 shows the noise density given for these parameters, which is derived from the white frequency noise representing ground-system frequency instability (see Section III.B).
- (3) Three stochastic parameters were included in the ground system error model to account for dynamical uncertainties in the Earth’s pole location and rotation period and to represent the pole model solutions developed by Finger and Folkner [17].

Table 5. Standard consider-state orbit determination filter with ground-system error model representative of current DSN calibration accuracy.

Estimated parameter set	Uncertainty (1σ)	Remarks
Spacecraft epoch state	A priori	Constant parameters
Position	10^3 km	
Velocity	1 km/s	
Nongravitational force model		
Solar radiation pressure	Steady-state	Markov parameters
Specular/diffuse reflectivity	10 percent of nominal	0.25–3 day time constant
Anomalous accelerations	Steady-state	Markov parameters
Radial	10^{-12} km/s ²	1–3 day time constant
Transverse	10^{-12} km/s ²	1–3 day time constant
Consider parameter set	Uncertainty (1σ)	Remarks
Ground system error model		
Station coordinates	A priori	Constant parameters
Spin radius (r_s)	0.18 m	
Z-height (z_h)	0.23 m	
Longitude (λ)	3.6×10^{-8} rad	
Geocenter offset	A priori	Constant parameter
Z-component	1 m	
Transmission media		
Zenith troposphere	A priori	Constant parameters
Wet	4 cm	
Dry	1 cm	
Gravitational force model		
Earth’s GM	A priori	Constant parameters
GM	$\text{GM} \times 10^{-8}$	
Harmonics	8×8 field (GEM-L2)	

- (4) The gravitational force model was the same model used in previous studies, with the Earth’s GM and truncated (8×8) GEM-L2 geopotential field harmonic coefficients treated as consider parameters. This is the only element of the overall enhanced filter model that used a standard consider state filtering approach.⁶

IV. Results

Results of the numerical error covariance analysis, based on data-acquisition and error-modeling assumptions described in Section III, are summarized in Table 6. The $1\text{-}\sigma$ position and velocity uncertainties for reconstructed orbit estimates are tabulated in a root-sum-square (RSS) sense for two different Doppler data-processing modes: (1) differenced-count Doppler data reduced with the standard consider state filter and (2) total-count phase data reduced with the enhanced filter.

The radio navigation performance results in Table 6 assume that science data were collected over the radio metric tracking data arcs. Accordingly, it appears that navigation performance is significantly improved with the more modern Doppler data-processing mode of total-count phase data reduced with

⁶ The argument for not treating the gravitational force model parameters as actual filter parameters is due principally to computational limitations when attempting to estimate the harmonic coefficients of the geopotential field (see discussion in Section II.B).

Table 6. Orbit accuracies of 1- σ for reconstruction over data arc.

Data-processing mode	VSOP	RadioAstron	ARISE (low)	ARISE (high)
	RSS position uncertainty, m			
Differenced-count Doppler with standard filter	12.6	10.9	11.5	83.5
Total-count phase with enhanced filter	5.5	6.5	6.5	30.0
RSS velocity uncertainty, cm/s				
Differenced-count Doppler with standard filter	0.17	0.03	0.26	0.41
Total-count phase with enhanced filter	0.06	0.02	0.13	0.15

the enhanced filter. However, these results reflect the accuracies that are achievable only over the specific data arcs and not over the entire orbit arcs. More precise representations of the reconstructed orbit accuracies over the entire orbit arcs (and in some cases over multiple orbit arcs) are shown in Figs. 1 through 4. These figures were constructed from filter-generated error covariances, which were smoothed and combined with consider parameter sensitivities to produce full consider covariances, then mapped forward to give a time history of the reconstructed position and velocity uncertainties over a 24- or 28-h period, depending on the sample orbit being evaluated.

From the time history plots (Figs. 1 through 4), a significant improvement in reconstructed orbit accuracies is seen when Doppler data are processed as phase-formulated measurements and reduced with the enhanced filter. This is true for both position and velocity uncertainties for all four sample orbits, with the most significant improvement evident in the perigee regions for velocity reconstruction, a regime that has historically met with limited success when using traditional radio metric data-processing methods.

Table 7 attempts to better quantify the performance improvement by giving both the range in uncertainties and the average (percentage) improvement over the 24- and 28-h time histories. Actual values used to generate the percentages of improvement were computed by integrating each error curve over the mapped interval to compare total areas of improved versus reference (conventional) data-processing modes. From this summary table, relative percentage improvements ranging from about 40 to 60 percent are seen, depending on the sample orbit. A slightly more dramatic improvement is seen for reconstructed velocity uncertainties over reconstructed positional uncertainties. Again, these results reflect the orbit accuracies over the entire propagation or mapping period, i.e., 24 h for the VSOP and both ARISE sample orbits and 28 h for the RadioAstron sample orbit.

Recall that the gravitational force model parameters assumed for both the standard and enhanced orbit determination filter models were treated as unmodeled consider parameters (see Tables 4 and 5). This was true for both GM and geopotential harmonic coefficients. To gain insight into the effect of these consider parameters on the filtering strategy being used, the approximate percentage contribution of these error sources on the total reconstructed position and velocity uncertainties over the propagation periods was computed, as illustrated in Fig. 5. The altitude dependence of the gravitational force modeling errors to the total reconstructed orbit accuracies is clearly evident. Not surprisingly, these errors contribute far more to the nontraditional data-processing mode; but this is an artifact of the filtering strategy being used and not the formulation of the Doppler observable. These results suggest that if improved navigation accuracies are to be achieved when using the enhanced orbit determination filter, it may

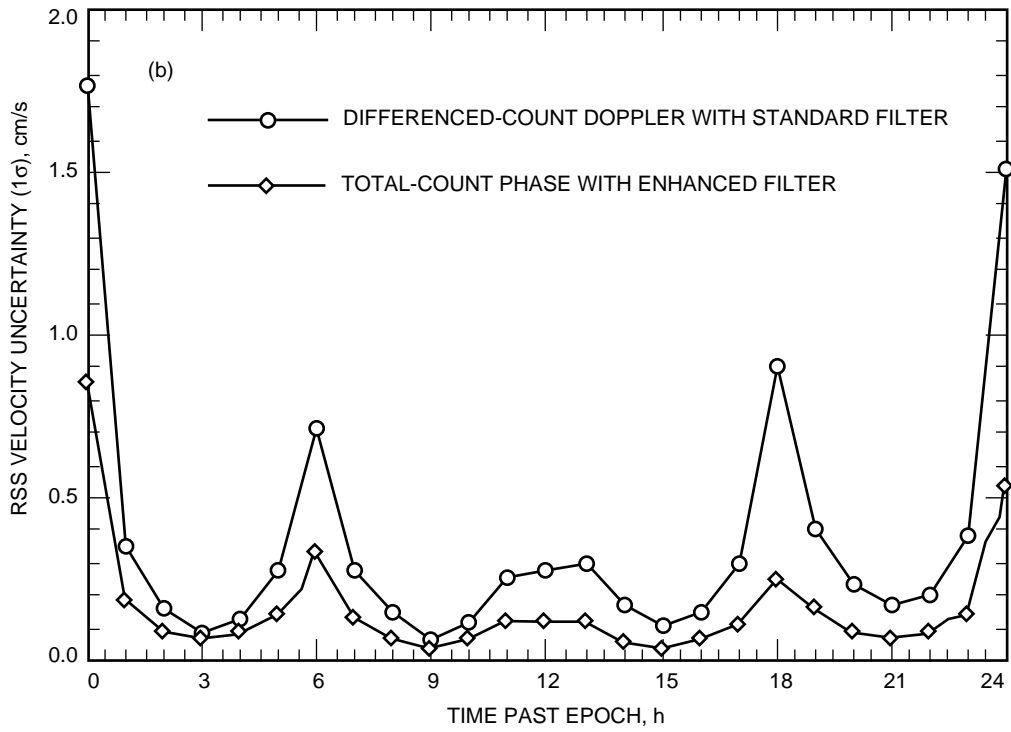
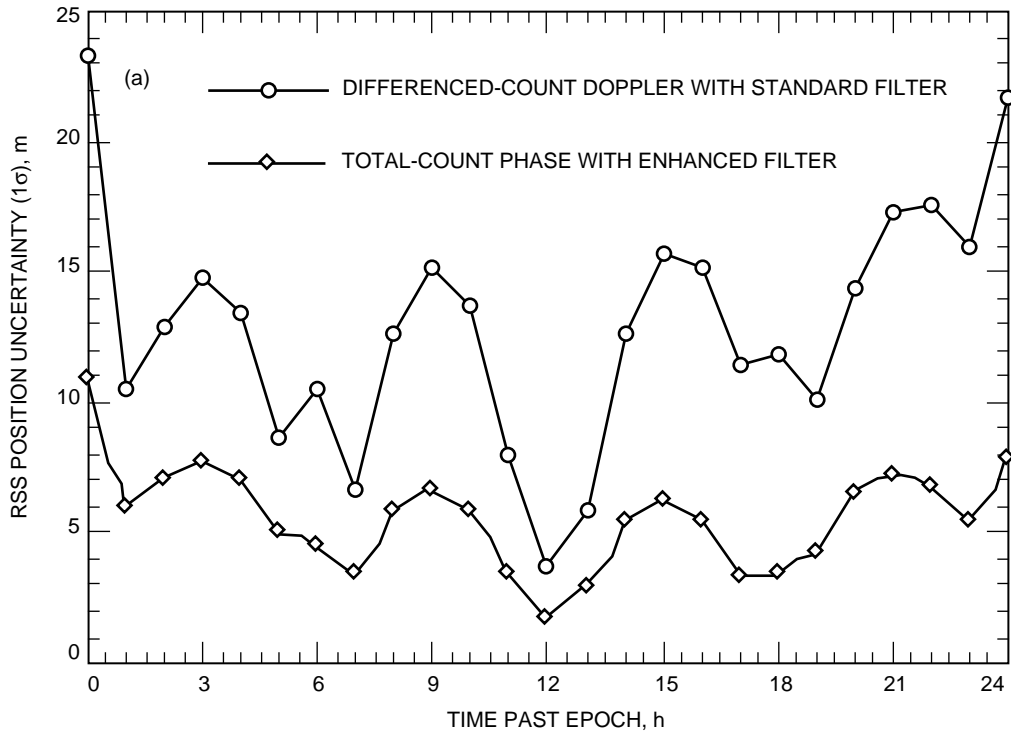


Fig. 1. VSOP 1- σ orbit determination accuracy statistics for expected RSS (a) total position uncertainty and (b) total velocity uncertainty.

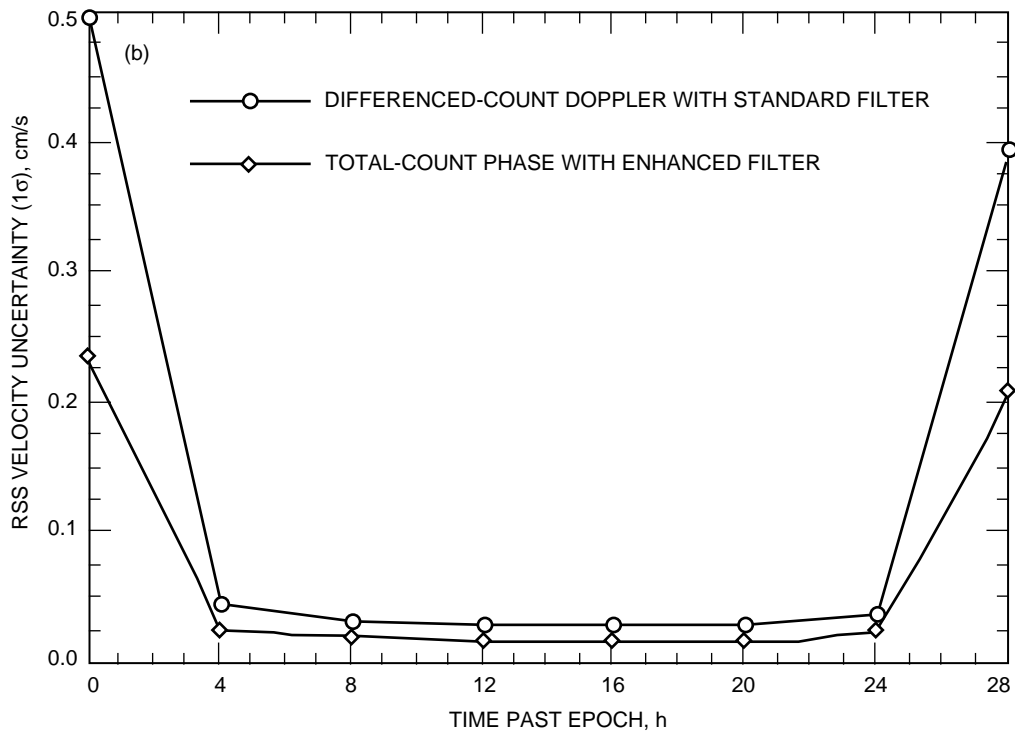
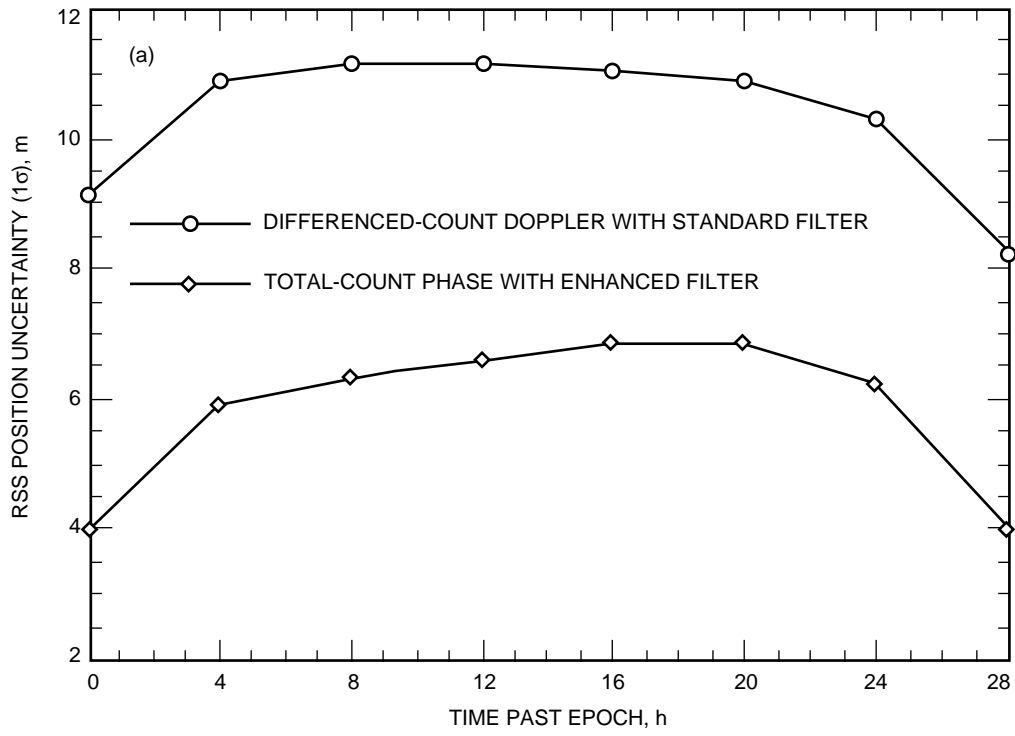


Fig. 2. RadioAstron 1- σ orbit determination accuracy statistics for expected RSS (a) total position uncertainty and (b) total velocity uncertainty.

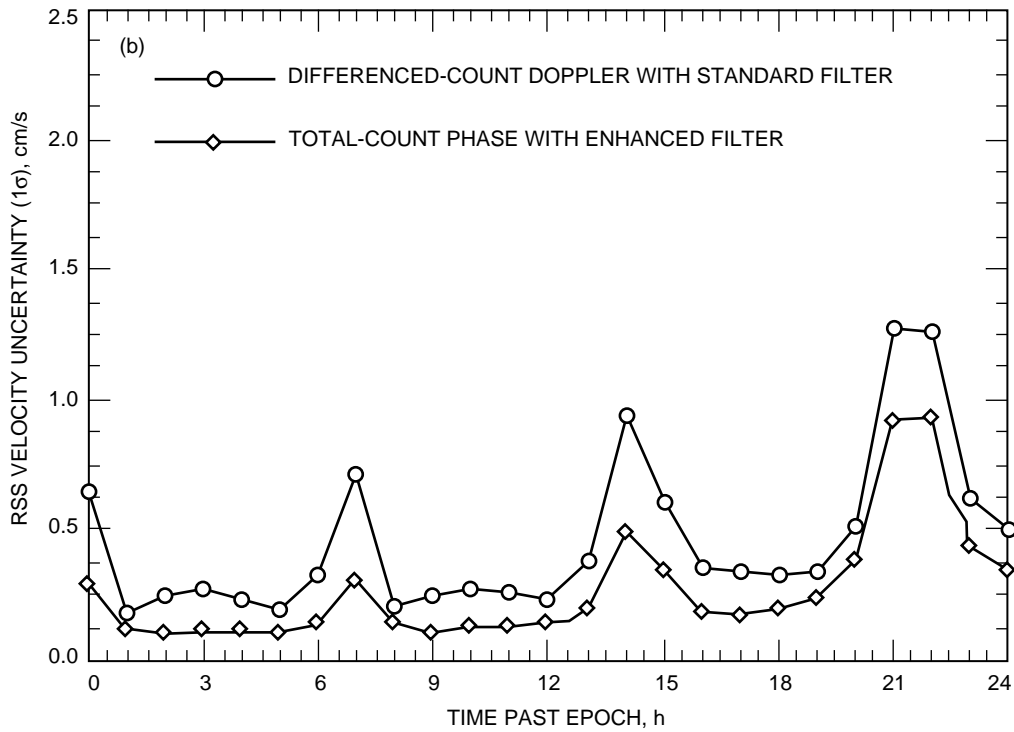
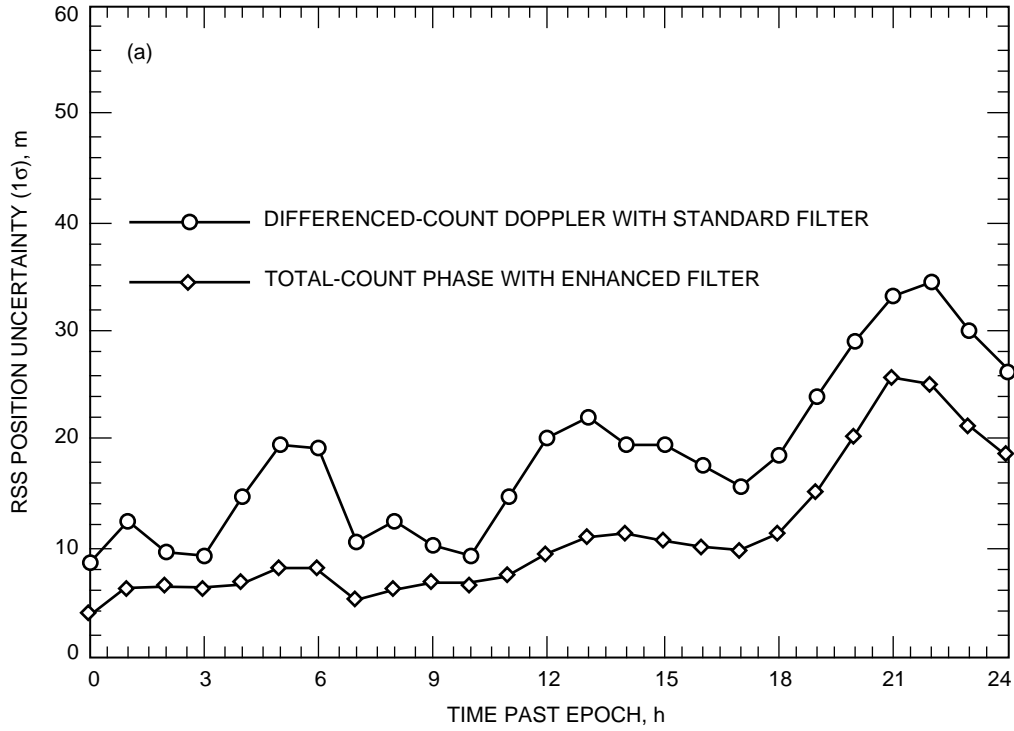


Fig. 3. ARISE (lower candidate orbit) 1- σ orbit determination accuracy statistics for expected RSS (a) total position uncertainty and (b) total velocity uncertainty.

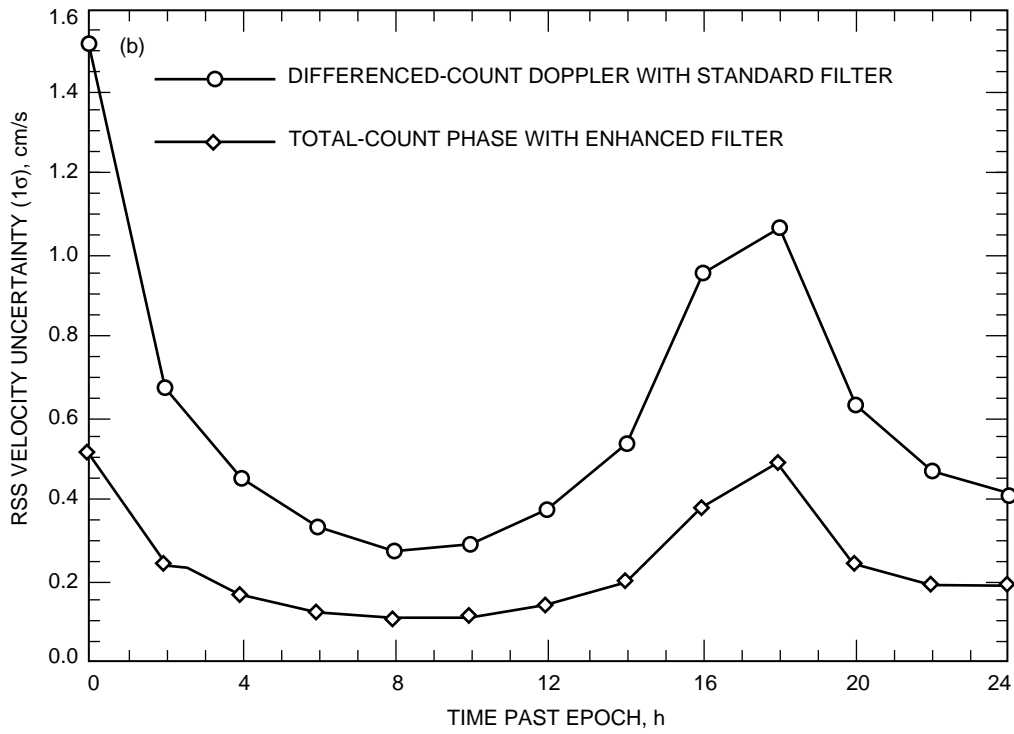
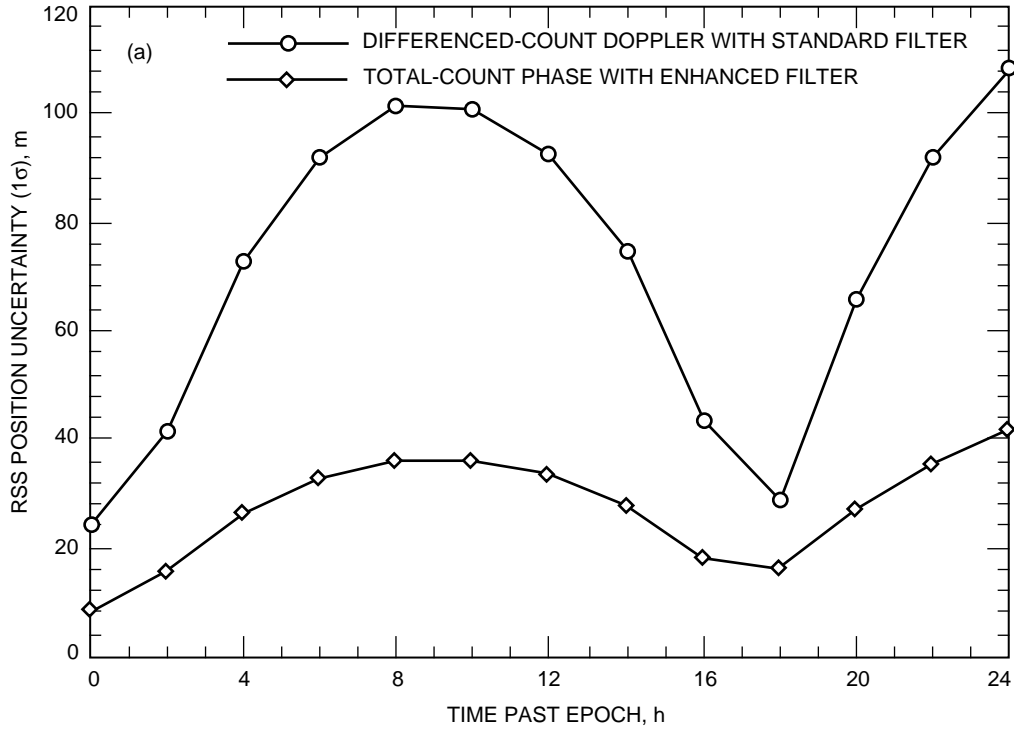


Fig. 4. ARISE (higher candidate orbit) 1- σ orbit determination accuracy statistics for expected RSS (a) total position uncertainty and (b) total velocity uncertainty.

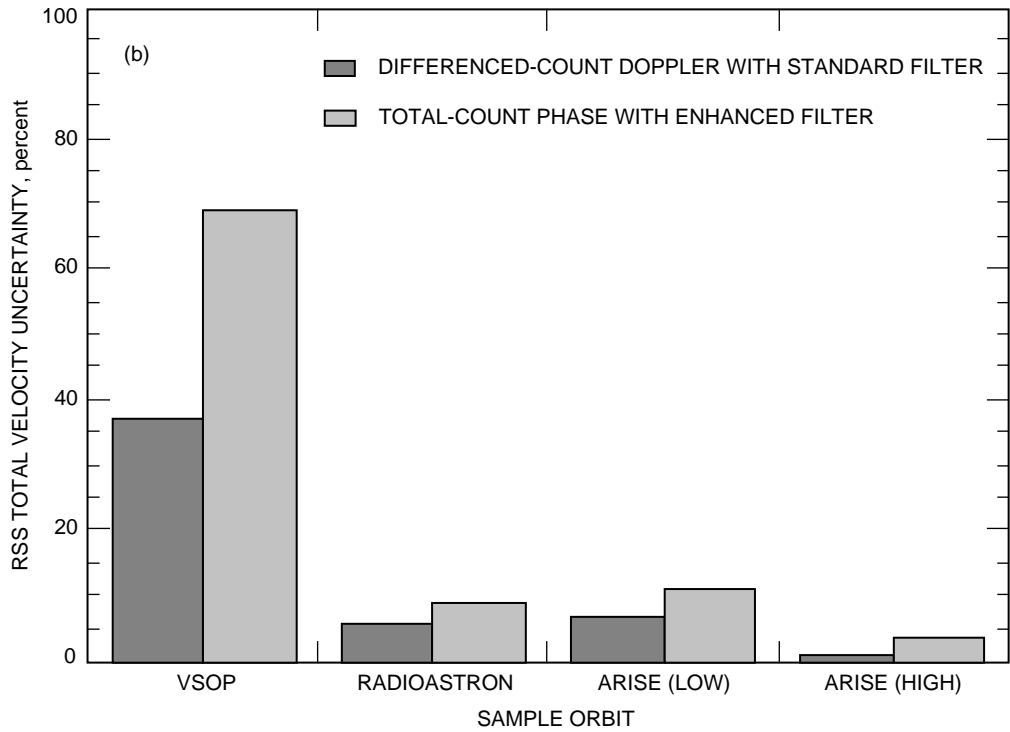
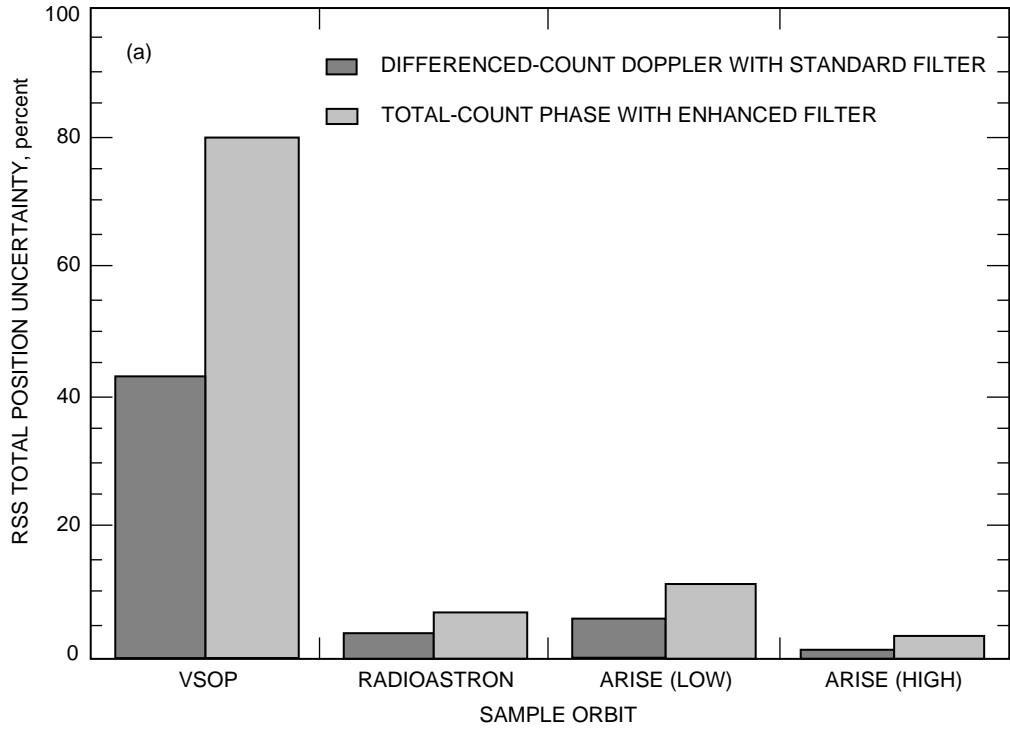


Fig. 5. Approximate percentage contribution of $1\text{-}\sigma$ gravitational force modeling errors (Earth GM and harmonics) to expected RSS (a) total position uncertainty and (b) total velocity uncertainty.

Table 7. Orbit accuracies of 1- σ for reconstruction over entire propagation period.

Data-processing mode	VSOP	RadioAstron	ARISE (low)	ARISE (high)
	RSS position uncertainty, m, and relative percentage improvement			
Differenced-count Doppler with standard filter	4–23	8–11	9–60	24–119
Total-count phaser with enhanced filter	2–11, 56 percent	4–7, 43 percent	4–49, 41 percent	8–48, 63 percent
RSS velocity uncertainty, cm/s, and relative percentage improvement				
Differenced-count Doppler with standard filter	0.06–1.8	0.03–0.5	0.2–2.4	0.3–1.5
Total-count phase with enhanced filter	0.03–0.9, 58 percent	0.02–0.2, 48 percent	0.1–2.0, 41 percent	0.1–0.5, 62 percent

be necessary to more accurately model the gravitational error sources and possibly treat the relevant parameters as actual filter parameters to be estimated along with the spacecraft trajectory parameters. The principal motivating factor for using a more sophisticated filtering strategy ultimately depends on mission requirements, bearing in mind the altitude dependence of gravitational force modeling errors.

V. Discussion

Although the results from two other possible permutations of candidate Doppler data-processing modes were not presented—e.g., differenced-count Doppler with enhanced filter and total-count phase with standard filter—error covariance calculations performed for these special cases reflect mixed performance results. Phase data reduced with the standard filter actually exhibited about a 40-percent worse orbit accuracy than traditional frequency-formulated Doppler with the standard filter because the precision of these data is very high and, thus, extremely sensitive to unmodeled ground-system calibration errors. As studies of interplanetary trajectories have shown, it is necessary to incorporate major ground-system calibration errors affecting the data as filter parameters to take full advantage of Doppler phase (without artificially deweighting the data).

When differenced-count Doppler data were used exclusively and reduced with the enhanced filter, there was a modest improvement in reconstructed orbit accuracies (~ 20 percent). However, it is imprudent to use this more complicated filtering strategy for very little gain, unless actual orbit determination requirements can be easily met.

Because of the long data arc lengths assumed for the higher orbits considered in this study, concern arose as to whether the presence of broken tracking passes might significantly degrade total-count phase navigation performance. Therefore, additional error covariance calculations were made for the RadioAstron orbit case. The phase passes were broken into three shorter intervals of equal length with a 5-min break between passes. This resulted in a net loss of about 15 min of data from the original case. An independent phase offset parameter was assumed for each pass and the covariance matrix reset at the beginning of each track to represent a Doppler count initialization procedure at each station, effectively yielding a new phase offset for each pass [1]. Results from this modified tracking scenario exhibited no marked degradation in reconstructed orbit accuracies from the original case, despite a 15-min reduction

in overall data arc length. This result clearly illustrates the robustness of the enhanced filter to solve for additional offset parameters incurred from a data-acquisition scenario involving broken tracking passes.

VI. Conclusions

A revised navigation error covariance analysis was performed for four highly elliptical Earth orbiters derived from the SVLBI mission set. This new study focused on utilizing recently developed or enhanced Doppler data-processing modes to reduce X-band Doppler data acquired from DSN-based radio tracking stations. Preliminary error analysis suggests a factor of 2 to 4 improvement in orbit accuracies is achievable over traditional data-processing modes when Doppler data are formulated as total-count phase measurements rather than differenced-count frequency measurements and processed with an enhanced data-filtering strategy that incorporates the major ground-system calibration error sources affecting the data as filter parameters.

Future work in this area will focus on a thorough sensitivity analysis to determine which dynamic and observational sources of error will require further modeling improvement or additional calibration accuracy. Plans for concept demonstrations are also being drafted that will use actual DSN-based radio-metric tracking data acquired during past mission operations in support of highly elliptical Earth-orbiting spacecraft. The JPL operational orbit determination software set is currently undergoing verification and validation tests for new upgrades that will facilitate the use of phase-formulated Doppler observables for use in both interplanetary and Earth-orbiter mission navigation support.

Acknowledgment

The author would like to thank J. Ellis for providing valuable input in preparation of this article.

References

- [1] S. W. Thurman and J. A. Estefan, "Radio Doppler Navigation of Interplanetary Spacecraft Using Different Data Processing Modes," *Advances in the Astronautical Sciences*, vol. 82, part II, pp. 985–1004, 1993.
- [2] J. A. Estefan, V. M. Pollmeier, and S. W. Thurman, "Precision X-Band Doppler and Ranging Navigation for Current and Future Mars Exploration Missions," *Advances in the Astronautical Sciences*, vol. 84, part I, pp. 3–16, 1993.
- [3] T. P. McElrath, S. W. Thurman, and K. E. Criddle, "Navigation Demonstrations of Precision Ranging with the Ulysses Spacecraft," *Advances in the Astronautical Sciences*, vol. 85, part II, pp. 1635–1650, 1993.
- [4] S. Bhaskaran, S. W. Thurman, and V. M. Pollmeier, "Demonstration of a Precision Data Reduction Technique for Navigation of the Galileo Spacecraft," Paper AAS 94-164, AAS/AIAA Spaceflight Mechanics Meeting, Cocoa Beach, Florida, February 14–16, 1994.
- [5] T. D. Moyer, *Mathematical Formulation of the Double-Precision Orbit Determination Program*, Technical Report 32-1527, Jet Propulsion Laboratory, Pasadena, California, pp. 72–80, May 15, 1971.

- [6] D. W. Curkendall, "Orbit Accuracy as a Function of Doppler Sample Rate for Several Data Taking and Processing Modes," *JPL Space Programs Summary 37-38*, vol. III, Jet Propulsion Laboratory, Pasadena, California, pp. 20–24, January–February 1966.
- [7] G. J. Bierman, *Factorization Methods for Discrete Sequential Estimation*, San Diego, California: Academic Press, Inc., pp. 162–171, 1977.
- [8] S. R. McReynolds, "The Sensitivity Matrix Method for Orbit Determination Error Analysis, With Applications to a Mars Orbiter," *JPL Space Programs Summary 37-56*, vol. 3, January–February 1969, Jet Propulsion Laboratory, Pasadena, California, pp. 85–87, March 31, 1969.
- [9] S. M. Lichten, "Estimation and Filtering Techniques for High-Accuracy GPS Applications," *The Telecommunications and Data Acquisition Progress Report 42-97*, January–March 1989, Jet Propulsion Laboratory, Pasadena, California, pp. 1–20, May 15, 1989.
- [10] D. J. Scheeres, "Failure Modes of Reduced-Order Orbit Determination Filters and Their Remedies," *The Telecommunications and Data Acquisition Progress Report 42-114*, April–June 1993, Jet Propulsion Laboratory, Pasadena, California, pp. 34–42, August 15, 1993.
- [11] J. A. Estefan and P. D. Burkhart, "Enhanced Orbit Determination Filter Sensitivity Analysis: Error Budget Development," *The Telecommunications and Data Acquisition Progress Report 42-116*, October–December 1993, Jet Propulsion Laboratory, Pasadena, California, pp. 24–36, February 15, 1994.
- [12] W. C. Masters, "Enhanced Orbit Determination Filter: Inclusion of Ground System Errors as Filter Parameters," *The Telecommunications and Data Acquisition Progress Report 42-116*, October–December 1993, Jet Propulsion Laboratory, Pasadena, California, pp. 37–41, February 15, 1994.
- [13] J. A. Estefan, "Precise Orbit Determination of High-Earth Elliptical Orbiters Using Differenced Doppler and Range Measurements," *The Telecommunications and Data Acquisition Progress Report 42-106*, April–June 1991, Jet Propulsion Laboratory, Pasadena, California, pp. 1–22, August 15, 1991.
- [14] T. Ichikawa and T. Kato, "Orbit Determination for MUSES-B Mission," Paper ISTS 94-c-21, 19th International Symposium on Space Technology and Science, Yokohama, Japan, May 15–24, 1994.
- [15] J. Ellis, "Navigation of Space VLBI Missions: Radioastron and VSOP," *Proceedings of the Second International Symposium on Ground Data Systems for Space Mission Operations*, JPL Publication 93-5, Jet Propulsion Laboratory, Pasadena, California, pp. 625–628, March 1, 1993.
- [16] J. S. Ulvestad, R. P. Linfield, and J. G. Smith, "ARISE: The Next Generation Space VLBI Mission," Paper AIAA 95-0824, 33rd Aerospace Sciences Meeting and Exhibit, Reno, Nevada, January 9–12, 1995.
- [17] M. H. Finger and W. M. Folkner, "A Determination of the Radio-Planetary Frame Tie From Comparison of Earth Orientation Parameters," *The Telecommunications and Data Acquisition Progress Report 42-109*, January–March 1992, Jet Propulsion Laboratory, Pasadena, California, pp. 1–21, May 15, 1992.